Emission estimates of HCFCs and HFCs in California from the 2010 CalNex study

Barbara Barletta,[1] Marc Carreras-Sospedra,[2] Alex Cohan,[2] Paul Nissenson,[3] Donald Dabdub,[2] Simone Meinardi,[1] Elliot Atlas,[4] Rich Lueb,[4,5] John S. Holloway,[6,7] Thomas B. Ryerson,[6] James Pederson,[8] Richard A. VanCuren,[9] and Donald R. Blake[1]

Received 20 June 2012; revised 20 December 2012; accepted 19 January 2013; published 25 February 2013.

[1] The CalNex 2010 (California Research at the Nexus of Air Quality and Climate Change) study was designed to evaluate the chemical composition of air masses over key source regions in California. During May to June 2010, air samples were collected on board a National Oceanic and Atmospheric Administration (NOAA) WP-3D aircraft over the South Coast Air Basin of California (SoCAB) and the Central Valley (CV). This paper analyzes six effective greenhouse gases—chlorodifluoromethane (HCFC-22), 1,1-dichloro-1-fluoroethane (HCFC-141b), 1-chloro-1,1-difluoroethane (HCFC-142b), 2-chloro-1,1,1,2-tetrafluoroethane (HCFC-124), 1,1,1,2-tetrafluoroethane (HFC-134a), and 1,1-difluoroethane (HFC-152a)—providing the most comprehensive characterization of chlorofluorocarbon (CFC) replacement compound emissions in California. Concentrations of measured HCFCs and HFCs are enhanced greatly throughout the SoCAB and CV, with highest levels observed in the SoCAB: 310 ± 92 pptv for HCFC-22, 30.7 ± 18.6 pptv for HCFC-141b, 22.9 ± 2.0 pptv for HCFC-142b, 4.86 ± 2.56 pptv for HCFC-124, 109 ± 46.4 pptv for HFC-134a, and 91.2 ± 63.9 pptv for HFC-152a. Annual emission rates are estimated for all six compounds in the SoCAB using the measured halocarbon to carbon monoxide (CO) mixing ratios and CO emissions inventories. Emission rates of 3.05 ± 0.70 Gg for HCFC-22, 0.27 ± 0.07 Gg for HCFC-141b, 0.06 ± 0.01 Gg for HCFC-142b, 0.11 ± 0.03 Gg for HCFC-124, 1.89 ± 0.43 Gg for HFC-134a, and 1.94 ± 0.45 Gg for HFC-152b for the year 2010 are calculated for the SoCAB. These emissions are extrapolated from the SoCAB region to the state of California using population data. Results from this study provide a baseline emission rate that will help future studies determine if HCFC and HFC mitigation strategies are successful.

Citation: Barletta, B., et al. (2013), Emission estimates of HCFCs and HFCs in California from the 2010 CalNex study, *J. Geophys. Res. Atmos.*, *118*, 2019–2030, doi:10.1002/jgrd.50209.

All supporting information may be found in the online version of this article.

[1]Department of Chemistry, University of California, Irvine, California, USA.
[2]Department of Mechanical and Aerospace Engineering, University of California, Irvine, California, USA.
[3]Department of Mechanical Engineering, California State Polytechnic University, Pomona, California, USA.
[4]Rosenstiel School of Marine and Atmospheric Science, University of Miami, Miami, Florida, USA.
[5]Atmospheric Chemistry, NCAR, Boulder, Colorado, USA.
[6]Chemical Sciences Division, NOAA/ESRL, Boulder, Colorado, USA.
[7]Cooperative Institute for Research in Environmental Sciences (CIRES), Boulder, Colorado, USA.
[8]Research Division, California Air Resources Board, Sacramento, California, USA.
[9]Air Quality Research Center, University of California, Davis, California, USA.

Corresponding author: B. Barletta, University of California, Irvine, Irvine, CA 92697, USA. (bbarlett@uci.edu)

2169-897X/13/10.1002/jgrd.50209

1. Introduction

[2] Chlorofluorocarbons (CFCs), hydrochlorofluorocarbons (HCFCs), and hydrofluorocarbons (HFCs) are anthropogenic compounds with chemical properties ideal for refrigerants (in both stationary and mobile air conditioning systems), foam-blowing agents, propellants, and degreasing solvents [*Sturrock et al.*, 2002; *McCulloch et al.*, 2001, 2003; *Derwent et al.*, 2007]. The ozone depletion potential (ODP) of CFCs and HCFCs led to their regulation under the Montreal Protocol and subsequent amendments [*UNEP*, 2003; *WMO*, 2011]. CFCs were completely phased out in developed nations by 1996 (with exceptions for essential uses, such as medical aerosols) and in "Article 5" nations (i.e. developing nations as defined by the Montreal Protocol) by 2010 [*UNEP*, 2003]. HCFCs have significantly lower ODP values than CFCs (Table 1) but still pose a threat to stratospheric ozone. HCFCs are viewed as transitional compounds and are scheduled to be completely phased out in developed nations by

Table 1. Chemical and Physical Characteristics of the HCFCs and HFCs Examined in This Study [*WMO*, 2011]. CFC-11 and CFC-12 Are Included for Comparison.

Common Name	Chemical Formula	Lifetime (year)	GWP (100 year)	ODP
HCFC-22	$CHClF_2$	11.0	1,790	0.055
HCFC-141b	CH_3CCl_2F	9.2	717	0.11
HCFC-142b	CH_3CClF_2	17.2	2,220	0.065
HCFC-124	$CHClFCF_3$	5.9	619	0.02–0.04
HFC-134a	CH_2FCF_3	13.4	1,370	–
HFC-152a	CH_3CHF_2	1.5	133	–
CFC-11	CCl_3F	45	4,750	1.0
CFC-12	CCl_2F_2	100	10,900	1.0

2030 (2040 for Article-5 nations; http://www.epa.gov/ozone/title6/phaseout/index.html).

[3] Hydrofluorocarbons do not harm the stratospheric ozone layer and are used as replacement compounds for both CFCs and HCFCs. However, HFCs (along with CFCs and HCFCs) have high global warming potentials (GWPs) due to their long lifetimes and strong ability to absorb infrared radiation [*Sihra et al*., 2001; *Forster and Joshi*, 2005; *Forster et al*., 2007]; the GWP of HFCs and HCFCs investigated in this study are orders of magnitude greater than carbon dioxide (CO_2) (Table 1). Because of the high GWP of HFC-134a (1,1,1,2-tetrafluoroethane, CH_2FCF_3), the main refrigerant used in automobile air conditioners [*McCulloch et al*., 2003; *Papasavva et al*., 2009], the European Union set a total ban in this compound in 2017 with a phase out in new vehicles starting in 2011[*EP*, 2006; *Henne et al*., 2012].

[4] Greenhouse gas (GHG) emissions are of particular interest to the state of California as it is the fifteenth largest emitter of GHGs worldwide (~2% of global emissions [*CARB*, 2008]). In September 2006, Assembly Bill 32 (AB 32, the Global Warming Solutions Act of 2006) was signed into law to address GHG emissions from California [*CARB*, 2008]. This law requires the California Air Resources Board (CARB) to develop regulations to reduce California's GHG emissions to 1990 levels by the year 2020. If successful, AB 32 will reduce GHG emissions down to 422 million metric tons of carbon dioxide equivalent ($MMTCO_2eq$; amount of CO_2 released into the atmosphere that would have the same warming influence as a given pulse emission of another greenhouse gas integrated over a specific time scale, commonly set to 100 years) by 2020, a 15% reduction from 2002 to 2004 levels (496 $MMTCO_2eq$) and a 30% reduction from the "business-as-usual" scenario projected for 2020 (596 $MMTCO_2eq$). The main strategies California will employ to achieve the 2020 GHG emissions target are included in the scoping plan approved by CARB on December 2008 (http://arb.ca.gov/cc/scopingplan/scopingplan.htm) and are scheduled to be implemented by 2012.

[5] It is necessary to establish baseline emission rates for HCFCs and HFCs in order to determine if the GHG mitigation strategies in AB 32 are successful. This study provides emission estimates of the most widely used HCFCs (HCFC-22, $CHClF_2$; HCFC-142b, CH_3CClF_2; HCFC-141b, CH_3CCl_2F; and HCFC-124, $CHClFCF_3$) and HFCs (HFC-134a and HFC-152a, CH_3CHF_2) in California for 2010. The emission rates of the six halocarbons are determined through a top-down method (named the "tracer ratio" method). This method utilizes atmospheric measurements collected over California during the CalNex campaign in May and June 2010, which was sponsored by CARB and the National Oceanic and Atmospheric Administration (NOAA). CalNex was designed as a multiinstitutional intensive field campaign focused on the interaction between air quality and climate change over California (http://www.esrl.noaa.gov/csd/projects/calnex).

[6] In the tracer ratio method–measured halocarbon/carbon monoxide (CO) concentration ratios are combined with inventory-base CO emission rates obtained from CARB (http://www.arb.ca.gov/ei/emissiondata.htm) to determine halocarbon emission rates for 2010. Air samples were collected over California, with most measurements obtained within three large source regions (Figure 1): (1) the South Coast Air Basin (SoCAB); (2) the part of the Central Valley (CV) north of the Sacramento-Joaquin River Delta, named the Sacramento Valley (SV); (3) the part of CV below 38.0°N, named the San Joaquin Valley (SJV). Additional samples were collected over the Pacific Ocean and are used to determine inflow concentrations. Halocarbon concentrations in the CV and SoCAB are affected by local emission sources as well as prevailing wind patterns, topography, and the presence of strong inversion layers. In the daytime during the summer, westerly winds from the Pacific Ocean enter the CV through the Carquinez Strait and diverge northward into the SV and southward into the SJV. Mountain ranges surrounding the CV, combined with a low altitude inversion layer, hinder the dispersion of air masses from the CV [*Zaremba and Carroll*, 1999; *Zhong et al*., 2004]. Similarly in the SoCAB, mountain ranges to the north and east of the basin and a low altitude inversion layer trap air masses brought in from the westerly winds [*Boucouvala and Bornstein*, 2003].

[7] Previous studies also have used the tracer ratio method to estimate halocarbon emissions from the SoCAB; *Barletta et al*. [2011] report emission rates of HFC-134a and HFC-152a during 2008 and *Gentner et al*. [2010] report emission rates of HCFC-141b during 2005. In the present work, population data are used to extrapolate halocarbon emission rates for the SoCAB during 2010 to the entire state of California. The results from this study also are compared with bottom-up emission inventories developed by CARB to assist with the validation of those estimates.

[8] A computer modeling study was conducted using the Community Multiscale Air Quality model (CMAQ; http://www.cmaq-model.org/) along with the Weather Research and Forecasting model (WRF; http://www.wrf-model.org/index.php) to examine the CO and halocarbon source collocation assumption used in the tracer ratio methodology.

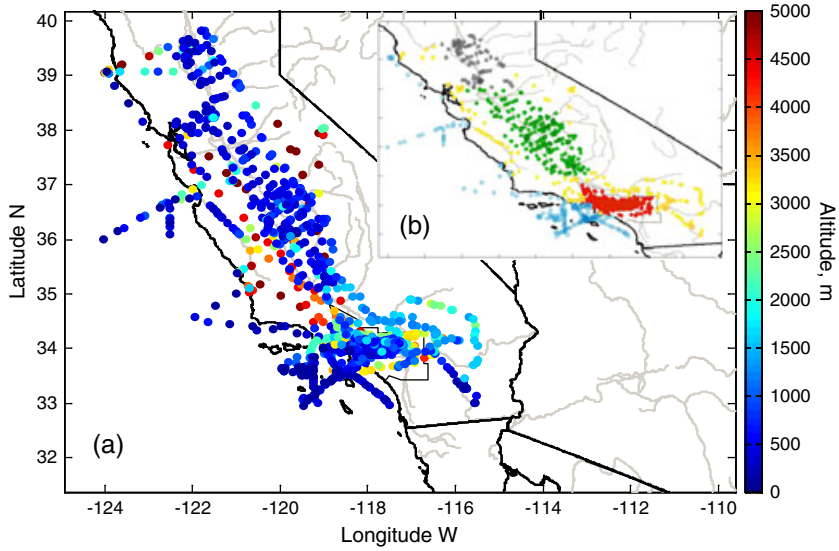

Figure 1. The location of samples collected over California during the CalNex 2010 campaign color-coded by altitude (a) and region (b). In Figure 1b, the regions examined are over the ocean (blue), SoCAB (red), SV (gray), SJV (dark green), and other (yellow).

2. Methodology

2.1. Collection of Air Samples and Analytical Method

[9] A total of 1,287 whole air samples were collected during 20 flights between 4 May and 21 June 2010 aboard a NOAA WP-3D aircraft stationed at Ontario, California. The flight plans were designed to provide the overall representation of the composition of the lower troposphere over California. Particular emphasis is placed on three large source regions—the South Coast Air Basin, the Sacramento Valley, and the San Joaquin Valley—with almost 80% of the samples collected at altitudes below 2 km (Figure 1). Inflow boundary conditions were determined using samples obtained over the Pacific Ocean.

[10] Polluted air masses can be transported great distances in the free troposphere, complicating source identification [*Liu et al*., 2003; *Barletta et al*., 2009]. However, air samples obtained within the planetary boundary layer (~0–2 km) [*Millet et al*., 2009] are strongly influenced by local sources. For this reason, the present study only uses samples collected below 2 km in estimating HCFC and HFC emissions, although samples were obtained at altitudes up to 6.6 km.

[11] Air samples in this study were collected using a similar methodology to *Barletta et al*. [2009] and *Barletta et al*. [2011]. Electropolished stainless steel canisters (1.3 L volume) with pneumatically controlled inlet valves were built into modules containing 12 canisters each, with six modules used during each flight. Prior to use in the field, the canisters were flushed with ultrahigh purity (UHP) helium and evacuated to 10^{-2} Torr. The internal walls were passivated by adding 17 Torr of water vapor from degassed ultrapure Milli-Q water, minimizing the adsorption of sample constituents inside the canisters. During the field measurements, the canisters were pressurized to 50 psia with ambient air using a two-stage metal bellows pump. Sample collection time was a function of altitude and lasted 5–25 s (a maximum of 72 canisters were filled for each flight). The contents of the canisters were analyzed at University of California, Irvine, within 7 days of sample collection using a gas chromatographic (GC) system. A total of 102 gases were analyzed and reported in the official CalNex data set archive, including halocarbons, nonmethane hydrocarbons, alkyl nitrates, oxygenated compounds, and sulfur compounds.

[12] The GC analysis utilizes two electron capture detectors, two flame ionization detectors, and one quadrupole mass spectrometer detector. The reader is referred to *Barletta et al*. [2009] for a detailed description of the GC system used in this study. The precision of the measurements varies by mixing ratio and by compound: 2% for the HCFCs; 5% for HFC-134a; 10% for HFC-152a. The measurement accuracy also varies by compound: 10% for the HCFCs and HFC-152a; 5% for HFC-134a.

[13] The details of the standard preparation are discussed in *Barletta et al*. [2011]. Briefly, original standards in the range of 10–300 ppb (nominal) were made in-house, provided by collaborators, and purchased from Scott-Marrin. These standards are checked against a butane/benzene standard from the National Institute of Standards and Technology using an atomic emission detector. A calibration curve in the range of ambient concentrations is obtained from dynamic dilutions of the high concentration standards and injection of variable volumes of these dilutions.

[14] CO was measured in situ on the WP-3D by a vacuum ultraviolet (VUV) fluorescence instrument [*Holloway et al*., 2000] with a precision of 2 ppbv and 5% accuracy.

2.2. Air Quality Modeling

[15] The CMAQ model was employed to help examine the tracer ratio methodology [*Byun and Ching*, 1999]. Specifically, the air quality model was used to analyze the assumption that halocarbon and CO sources were collocated within the SoCAB. CMAQ is a comprehensive air quality modeling system developed by the U.S. Environmental Protection Agency (US EPA) and is used in many regulatory air quality applications such as studying tropospheric ozone, particulate

matter, acid deposition and visibility [*Appel et al*., 2008, 2010; *Foley et al*., 2010]. In the present study, CMAQ was used to simulate the atmospheric concentrations of halocarbons resulting from direct emissions and transport in California during the time period corresponding to the CalNex campaign (1 May to 21 June 2010). The atmospheric lifetimes of the halocarbons examined in this study (~years, Table 1) are much greater than their residence times within California (~days). Therefore, chemical interaction of the halocarbons with other species was excluded in the simulations. The advection model in CMAQ is based on the Yamartino-Blackman Cubic Scheme [*Yamartino*, 1993], and vertical turbulent mixing is based on the K theory [*Chang et al*., 1987; *Hass et al*., 1991]. Meteorology for CMAQ was obtained from the Advanced Research Weather Research and Forecasting Model, WRF-ARW [*Skamarock et al*., 2005]. The National Centers for Environmental Prediction (NCEP) Final Operational Global Analysis $1^\circ \times 1^\circ$ grids data were used for WRF-ARW initial and boundary conditions.

[16] In the CMAQ model, halocarbon emissions were spatially and temporally resolved proportionally to CO emissions. It is expected that the modeled and observed halocarbon concentrations would exhibit similar spatial and temporal trends to be consistent with the assumption that CO and halocarbon emissions are collocated. The spatial and temporal distribution of halocarbon emissions were determined by multiplying the halocarbon/CO ratios obtained from aircraft measurements during the CalNex campaign (discussed in section 3.2) with gridded CO emissions for the SoCAB. The CO emission rates were developed by CARB for a typical 1-week period for the summer of 2008 [*Huang et al*., 2011] and scaled to 2010 levels using emission trends from CARB (http://www.arb.ca.gov/app/emsinv/fcemssumcat2009.php). The 1-week emission pattern is repeated for all 8 weeks of the modeling period. Supplementary Figure 1 shows daily midweek CO emissions across California, with the largest CO source regions being the SoCAB, San Francisco Bay Area, and SV.

3. Results

3.1. Spatial Distribution in Measured Halocarbon Concentrations

[17] Background levels of the four HCFCs and two HFCs examined in this study were determined by analyzing a total of 269 inflow air samples that were collected over the Pacific Ocean (Figure 1). As in *Barletta et al*. [2011], the average mixing ratio of the lowest quartile for the samples was used as the regional background level. Measurements of HCFCs and HFCs in the global tropospheric background are available through the Advanced Global Atmospheric Gases Experiment (AGAGE) network (http://agage.eas.gatech.edu/). Previous works have used these data to evaluate long trend atmospheric measurements of halocarbons and to infer global emission estimates [i.e., *Miller et al*., 1998; *Prinn et al*., 2000; *O'Doherty et al*., 2004; *Greally et al*., 2007]. The background concentrations obtained during the CalNex campaign (Table 2) are in good agreement with observations at the AGAGE remote monitoring station in Trinidad Head, California (41.05°N, 124.15°W; http://agage.eas.gatech.edu/data.htm) during June 2010. The difference between the background concentrations observed during the CalNex campaign and at Trinidad Head are less than 2% for HCFC-141b, ~7% for HFC-152a and HCFC-142b, and ~10% for HFC-134a and HCFC-141b (no data are available for HCFC-124 levels at Trinidad Head).

[18] As stated previously, most of the air samples were collected over three major source regions (Figure 1b): (1) SoCAB (385 samples), (2) SV (85 samples), and (3) SJV (206 samples). Additionally, 117 samples were obtained outside of these three areas; Table 2 lists the mean and standard deviation of the HCFC and HFC concentrations measured in the three source regions (SoCAB, SV, and SJV), in the inflow air mass, and in all other areas sampled. A *t* test comparing halocarbon concentrations from the three major source regions to the inflow concentrations indicates that almost all halocarbon species were significantly enhanced (at a 0.05 confidence level) in the source regions compared to the inflow air mass; only HCFC-141b and HCFC-124 in SV, and HCFC-141b in SJV do not differ significantly from background mixing ratios. The concentrations of all six CFC-replacements examined in this study were much higher in the SoCAB compared to the other regions (Figure 2).

[19] Halocarbon concentrations are affected by local emission sources, wind patterns, topography, and the presence of strong inversion layers. The effect of wind direction and speed on the distribution of halocarbon levels was examined for air samples in the bottom quartile ("cleanest" air samples) and the top quartile ("dirtiest" air samples). Figure 3 shows wind rose plots for HFC-152a, the compound most enhanced compared to background levels; similar wind

Table 2. The Mean, 1 Standard Deviation (SD), and Ranges for the Samples Collected Over Different Source Regions. Mixing Ratios Are in pptv.

	Background[a]	California ($n=793$)	SoCAB ($n=385$)		SV ($n=85$)		SJV ($n=206$)		Others ($n=117$)	
	Mean (SD)	Mean (SD)	Mean (SD)	Range	Mean (SD)	Range	Mean (SD)	Range	Mean (SD)	Range
HCFC-22	215 (3.0)	274 (76)	310 (92)	215–1068	240 (25)	213–315	235 (30)	209–602	250 (33)	213–480
HCFC-141b	19.4 (0.4)	26.5 (13.7)	30.7 (18.6)	18.7–216	22.1 (2.5)[b]	18.5–29.2	22.0 (2.7)[b]	18.5–37.4	23.7 (2.9)	19.2–31.7
HCFC-142b	20.2 (0.3)	22.2 (1.7)	22.9 (2.0)	19.7–37.7	21.8 (1.2)	20.2–25.7	21.3 (0.8)	19.9–25.1	21.7 (1.2)	19.6–27.7
HCFC-124	2.07 (0.27)	3.89 (2.11)	4.86 (2.56)	1.54–16.9	2.80 (0.60)[b]	1.52–4.10	2.98 (0.70)	1.53–5.08	3.10 (1.25)	1.55–10.5
HFC-134a	54.7 (1.0)	87.7 (39.7)	109 (46.4)	53.9–489	66.7 (13.7)	53.8–123	64.8 (10.3)	53.5–111	72.2 (15.7)	53.2–155
HFC-152a	8.50 (1.27)	57.3 (56.8)	91.2 (63.9)	8.71–317	23.9 (13.0)	9.23–57.7	21.5 (14.3)	7.33–94.1	32.5 (22.2)	9.51–129

[a]Background levels are the mean values of the lowest quartile of samples collected over the Pacific Ocean (the number of samples corresponding to the lowest quartile ranges from 59 samples to 68 samples; see section 3.1 for details).

[b]The concentrations of HCFC-141b and HCFC-124 in SV and HCFC-141b in SJV do not differ significantly from background levels at the 0.05 confidence level.

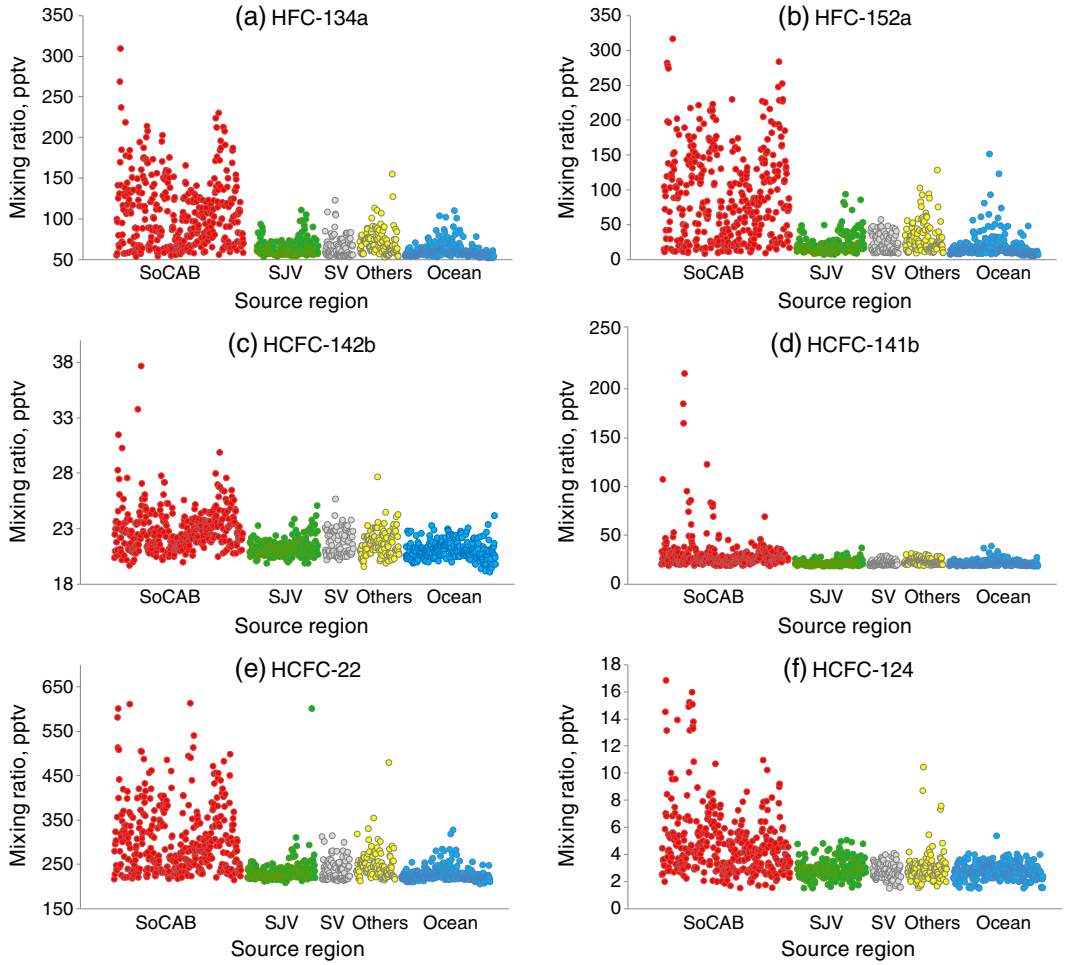

Figure 2. Mixing ratios of HFC-134a (a), HFC-152a (b), HCFC-142b (c), HCFC-141b (d), HCFC-22 (e), and HCFC-124 (f) measured over the SoCAB (red; 385 samples), the SJV (dark green; 206 samples), the SV (gray; 85 samples), all other California regions (yellow; 117 samples), and the ocean (blue; 269 samples). One outlier for HFC-134a (489 pptv) and two outliers for HCFC-22 (910 and 1068 pptv) are excluded from the plots. The width of the bins is proportional to the number of data points in each bin in order to better resolve the data points.

rose plots for HFC-134a and the other HCFCs are presented in Supplementary Figures 2–6. In both the SoCAB and SJV, the highest and lowest HCFC and HFC concentrations are measured when wind blows from the same general direction; there does not appear to be a correlation between concentration and wind direction in those two regions. However, the HCFC and HFC concentrations are highest in the SV when winds are predominantly from the SSE and lowest when winds are predominantly from the NNW, possibly indicating that HCFC and HFC emissions from the SJV, San Francisco area, and Sacramento River Delta play a role in determining halocarbon levels measured in the SV during the CalNex campaign.

3.2. Emission Estimates Using the Tracer Ratio Method

[20] In the tracer ratio method, the halocarbon emission rate is calculated by multiplying the measured halocarbon/CO concentration ratio in the region of interest with the reported CO emission rate in that region (obtained from CARB). The validity of this methodology is dependent upon four assumptions: (1) the halocarbon and CO sources are collocated; (2) the emission rate of CO is well known; (3) the lifetime of the chemical compounds is greater than the typical transport time (~days), which is valid for CO (lifetime ~ 2 months) [*Logan et al.*, 1981] and the halocarbons in the study (lifetime ~1.4–17.9 years; Table 1); (4) the enhancements due to recent emissions is large relative to other influences (latitudinal or vertical gradients associated with the source region of air reaching California, instrumental precision, seasonal variability, etc.). Numerous studies have used the tracer ratio method to estimate emissions of long-lived species [e.g., *Reimann et al.*, 2005; *Yokouchi et al.*, 2006; *Greally et al.*, 2007; *Hurst et al.*, 2006; *Millet et al.*, 2009; *Gentner et al.*, 2010, *Hsu et al.*, 2010, *Barletta et al.*, 2011].

[21] Figure 4 demonstrates that a good correlation exists between CO and all six halocarbons in the SoCAB (coefficient of determination, $R^2 = 0.41–0.86$), indicating that the anthropogenic sources responsible for the emissions of these compounds likely are collocated within this region. The halocarbon/CO molar ratio is determined from the slope of

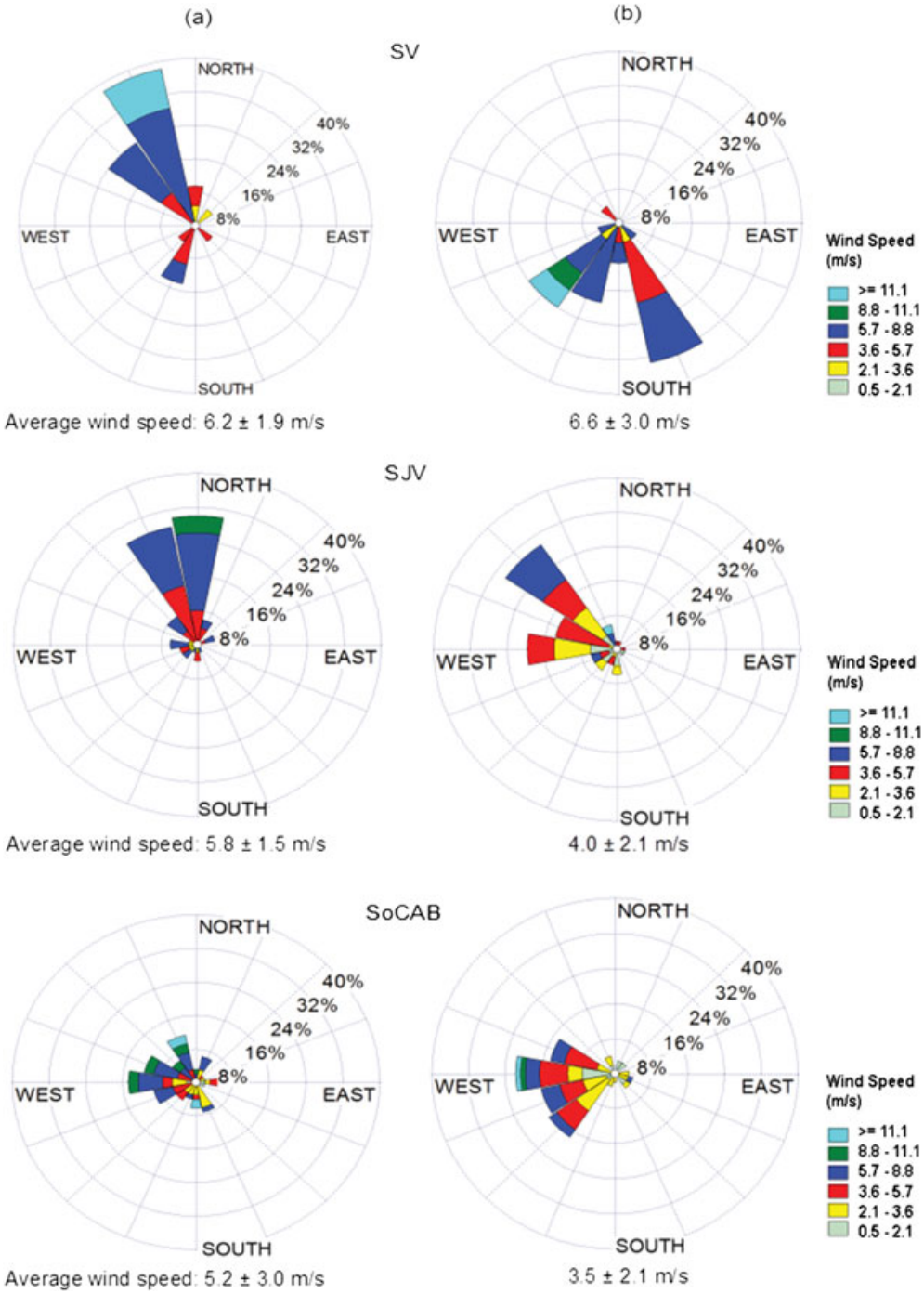

Figure 3. Sixteen-point wind roses computed using the lowest quartile (a) and the highest quartile (b) of HFC-152a samples collected over the SV (top), the SJV (middle), and the SoCAB (bottom). The fraction of wind coming from a specific direction is represented by the percentage value, while the wind speed is illustrated by the different color coding.

the orthogonal regression line and is converted into a mass ratio using the molecular weights of the different species. Statistical outliers (>98 percentile, corresponding to about 6% of the data) and two data points with negligible anthropogenic influence (CO mixing ratios of 97 and 104 ppbv, lower than the measured local background of 107 ppbv) are excluded from the regression analysis. The halocarbon/CO mass ratio is multiplied by the 2010 CO emission rate from the SoCAB, as determined by CARB (2,950 tons/d; http://www.arb.ca.gov/ei/emissiondata.htm) to obtain the emission rate of each of the six halocarbons in the SoCAB during the CalNex study. The 2010 CO emissions for the SoCAB are projected from the 2008 CO emissions inventory (3,249 tons/d), which is the latest emissions inventory available from CARB.

[22] The correlation between CO and the six halocarbons in the SV and SJV is relatively poor ($R^2 < 0.28$ for all halocarbons), indicating that the major CO and halocarbon

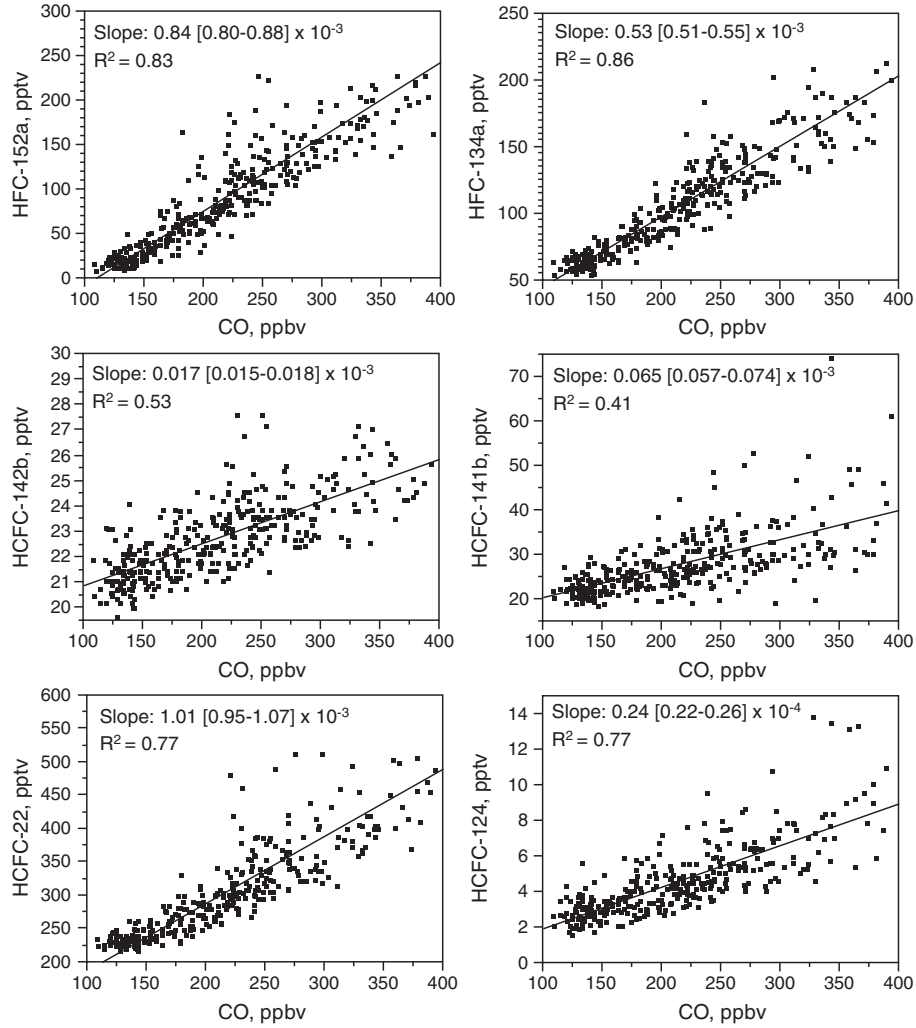

Figure 4. Halocarbon concentrations versus CO correlation plots observed for the samples collected over the SoCAB. The slope of the orthogonal distance regression line is reported with the 95% confidence level (in brackets).

sources likely are not collocated in those regions. Considering that most HCFC and HFC emissions are released from refrigeration and stationary and mobile air conditioning systems, HCFC and HFC emissions will be collocated with CO emissions related to residential and commercial activities and to transportation. In the SoCAB, transportation dominates CO emissions (light-duty trucks and passenger vehicles emit about 43% of CO in the SoCAB, but only 22% and 24% in the SV and SJV, respectively; http://www.arb.ca.gov/app/emsinv/emssumcat.php), and as a result, CO and halocarbon emissions are relatively well collocated as indicated by the regression analysis. According to the CARB, emissions from wildfires and managed burning (i.e., agricultural burning, forest management and weed abatement) add up to 31% and 35% of total CO emissions in the SJV and the SV, respectively. Those CO sources are located predominantly in rural areas, are widely dispersed, and are not associated with any halocarbon emission source. In contrast, CO emissions from wildfires and managed burning only contribute to 6% of total CO emissions in the SoCAB. The large contribution of such sources to CO emissions in the SJV and SV is deemed to be one of the causes for the poor correlation observed between CO and halocarbons in those two regions. Low R^2 values prevent the use of the tracer ratio method to determine halocarbon emission rates in the SV and SJV.

[23] The HCFC and HFC emission rates from the SoCAB are extrapolated to the entire state of California using population data. The methodology assumes that the per capita halocarbon emissions in a subregion apply to the larger region, a methodology used in previous works [e.g., *Millet and Goldstein*, 2004; *Li et al*., 2005; *Hurst et al*., 2006; *Stohl et al*., 2009; *Barletta et al*., 2011]. Extrapolating emission rates from the highly urbanized SoCAB to the state of California using population data also is consistent with the idea that urban areas dominate emissions of CFC replacements [*Hurst et al*., 2006]; the per capita halocarbon emission rate from the SoCAB likely is representative of the per capita halocarbon emission rate for the state. Moreover, as noted by *Stohl et al*. [2009], using population data to calculate global emissions estimates likely overpredicts emissions from developing countries, but this error decreases when the extrapolation is limited to an individual nation.

[24] The field measurements were obtained during the months of May and June 2010, and it is expected that both

halocarbon and CO emission rates vary with season. *Barnes et al*. [2003] observed a seasonal variability in the $\Delta X/\Delta CO$ ratio (X = CFC-12 and CFC-11) in the northeastern United States during 1996–1998 with higher slopes during the summer compared to the winter. Seasonal differences in emissions are expected to be less severe in Southern California than in the northeastern United States because of the lower temperature variability among seasons. In addition, spring temperatures usually are representative of the average annual temperature in the SoCAB; in 2010, the average annual temperature in Los Angeles was 17°C while the average temperature during May and June was 16°C and 18°C, respectively (http://www1.ncdc.noaa.gov/pub/orders/33F413D5-9457-4595-B163-8D7D027DA25F.pdf). Therefore, it is assumed that halocarbon emission rates calculated using the CalNex data likely are representative of the entire year and the seasonality correction factor is set to unity.

[25] The estimated emission rates and their uncertainty ranges for the six halocarbon compounds examined in this study are presented in Table 1. The uncertainty ranges are based on the uncertainty in (1) the halocarbon/CO slopes obtained from the orthogonal regression (listed in Figure 1), (2) the seasonality correction factor, and (3) the CO emissions. The seasonality error is determined by observing the variability in the spring-to-annual $\Delta X/\Delta CO$ (X = CFC-11, CFC-12) enhancement ratio measured by *Barnes et al*. [2003] for any 1 year with respect to the 3-year means, which is ±10%. The uncertainty in CO emissions is not provided by CARB and a value of ±20% is assumed for the year 2010. This value is determined by doubling the size of the scaling factor (about 10%) in the 2010 projection (2,950 tons/d) from to the 2008 CO emission inventory (3,249 tons/d), which is the latest emissions inventory available from CARB. The uncertainty in the CO estimate also was selected in light of the 20% error in the U.S. anthropogenic CO source assumed by *Millet et al*. [2009] to derive halocarbon emissions from the United States using the tracer ratio method. In computing statewide emissions, it is assumed that the emission ratio calculated from the observed halocarbon/CO slope in the SoCAB is representative throughout the state of California. This assumption follows from the idea that human activities in the SoCAB are very similar to areas with comparable climate and urban settings (such as San Diego or South Central Coast air basin) and that the same products, housing, and vehicles are used statewide. However, the halocarbon/CO emission ratios could be different in nonurban settings such as areas with heavy industrial activities or where agricultural emissions dominate. For this reason, an "extrapolation correction factor" is included in the calculation of statewide emission estimates. Because it is not possible to quantify how the emission ratio could change outside the SoCAB, this factor is set to unity with an uncertainty designed to supplement the overall error associated with California estimates. The error associated with the extrapolation correction factor for each halocarbon is determined by comparing the halocarbon/CO emission ratio in the SoCAB to a statewide average emission ratio. The emission ratio in the SoCAB is computed using the observed halocarbon/CO mixing ratio (Figure 1). The statewide average emission ratio is computed by assuming an emission ratio in regions outside the SoCAB and then calculating a weighted average by population. It is assumed that the emission ratio in the San Diego Air Basin, which has a population of 3.2 million, is the same as in the SoCAB since both regions have very similar climate and demographics. Regions outside the SoCAB and San Diego Air Basin are given an emission ratio that differs by 50% from the SoCAB emission ratio. The difference between the emission ratio calculated in the SoCAB and the statewide average emission ratio is approximately 25%, and this value is used to represent the uncertainty associated with the extrapolation correction factor. The statewide emissions listed in Table 1 include this additional uncertainty.

[26] The authors note that an additional error associated with population data should be considered when the SoCAB emissions are extrapolated to California. However, because uncertainty in the population data is not available, it is not included in the error range calculated for the California emissions estimates.

[27] Table 3 compares results from this study with estimates from previous studies that also use the tracer ratio method to calculate HFC and HCFC emission rates from the SoCAB. The HFC-134a and HFC-152a emission rates calculated for 2010 in this study (1.89 ± 0.43 and 1.94 ± 0.45 Gg yr^{-1}) are within the margin of error of the values calculated for 2008 by *Barletta et al*. [2011] (2.12 ± 0.28 and 1.60 ± 0.22 Gg yr^{-1} for HFC-134a and

Table 3. A Comparison of Previous Literature Data to the 2010 HCFC and HFC Emission Rates From the SoCAB and California (CA) Calculated From the CalNex Data Set and CARB

	SoCAB (Gg yr^{-1})			CA (Gg yr^{-1})		CA ($MMTCO_2eq$)
	Present Study[a]	CARB[b,c]	Literature	Present Study[a,d]	CARB[b,c]	Present Study[d]
HCFC-22	3.05 ± 0.70[e]	3.52		7.09 ± 2.41	8.17	12.8 ± 4.4
HCFC-141b	0.27 ± 0.07	0.25	0.18 ± 0.03[f]	0.63 ± 0.23	0.58	0.46 ± 0.17
HCFC-142b	0.06 ± 0.01	0.07		0.14 ± 0.04	0.17	0.32 ± 0.09
HCFC-124	0.11 ± 0.03	0.10		0.26 ± 0.10	0.22	0.16 ± 0.06
HFC-134a	1.89 ± 0.43	1.62	2.12 ± 0.28[g]	4.39 ± 1.48	3.76	6.3 ± 2.1
HFC-152a	1.94 ± 0.45	1.94	1.60 ± 0.22[g]	4.51 ± 1.54	4.49	0.56 ± 0.19

[a]Derived from measurements obtained during the CalNex campaign (May–June 2010).
[b]Inventory-based from Gallagher *et al*., 2012; manuscript in preparation.
[c]CARB estimates are statewide, bottom-up, emission estimates derived from usage rates in California.
[d]Extrapolated from SoCAB emissions estimates using population data.
[e]Uncertainties in emission estimates for the present study are discussed in section 3.2.
[f]*Gentner et al*. [2010] for 2005.
[g]*Barletta et al*. [2011] for 2008.

HFC-152a, respectively). The emission rate of HCFC-141b in the SoCAB was 0.18 ± 0.03 Gg yr^{-1} in 2005 [*Gentner et al*., 2010] and 0.27 ± 0.07 Gg yr^{-1} in 2010 (present study). While production and import of HCFC-141b was phased out in the United States. in 2003, finished products containing HCFC-141b can be imported legally into the United States, and limited production is allowed for legitimate needs. Despite these restrictions, the present study finds that HCFC-141b emissions possibly increased by 50% in California during 2005–2010 (we note that if the error ranges associated with the emission estimates are considered, the increase is less remarkable). The U.S. EPA also estimates that U.S. emissions of this compound increased greatly during a similar time period, from 4.2 Gg yr^{-1} in 2005 to 8.7 Gg yr^{-1} in 2010 [*EPA*, 2012]. Background levels of HCFC-141b rose during 2005–2010, as documented by the AGAGE measurements at Trinidad Head, California (19.4 ± 0.2 pptv in March 2005 and 22.1 ± 0.6 pptv in September 2010; http://agage.eas.gatech.edu/data_archive/agage/).

[28] The present study, *Gentner et al*. [2010], and *Barletta et al*. [2011] utilize a top-down method to calculate halocarbon emission rates in the SoCAB. Emission rates also may be calculated using bottom-up methodologies that are based on usage data. Bottom-up estimates of the halocarbons examined in this study are available from CARB and are listed in Table 1 [Gallagher *et al*., 2012, manuscript in preparation]. CFC and CFC replacement emission estimates from CARB are based primarily on California-specific emissions and are scaled down to smaller regions using population data. There is excellent agreement between CARB's bottom-up emissions estimates and the estimates from this study for HFC-152, HCFC-141b, and HCFC-124; CARB's estimates for these three species are well within this study's uncertainty ranges where we assumed a 20% error in the 2010 CO source. Although the discrepancies between the emission rates from CARB and this work for HFC-134a, HCFC-22, and HCFC-142b are greater, CARB's estimates still within the uncertainty ranges determined by this study. Given that bottom-up estimates can be affected significantly by uncertainties of industry and government reports, the top-down estimates calculated are consistent with the bottom-up estimates from CARB.

[29] The six halocarbon species examined in this study have GWPs ranging from 124 to 2310 (Table 1). In order to compare the relative warming influence of HCFC and HFC emissions with carbon dioxide emissions, the halocarbon emission rates calculated in this study are converted to $MMTCO_2eq$ by multiplying the emission rates with the 100 year GWP values listed in Table 1. As shown in Table 1, the four HCFCs and two HFCs are responsible for approximately 4.5% of the total emissions of GHGs from the state of California in 2010 (462 MMTCO2eq, http://www.arb.ca.gov/cc/inventory/data/forecast.htm).

3.3. Comparison of Observed and Modeled Concentrations

[30] The halocarbon emission fields for California used in the CMAQ model are calculated using CO emissions developed by CARB for a typical 1 week period during the summer of 2008. CO emissions in the SoCAB are scaled to 2010 levels using emissions trends from CARB and multiplied by the halocarbon/CO ratios observed during the CalNex study. The halocarbon/CO ratios from the SoCAB (<2 km) are used because measurements of halocarbons and CO are strongly correlated in that region (Figure 1), whereas the correlation is relatively poor in other areas. The 1 week emission pattern is repeated for all 8 weeks of the modeling period.

[31] The initial conditions for halocarbons were set to background levels for 1 May at midnight. The first measurements in the SoCAB were obtained on 4 May, at noon, which allowed for an effective model spin-up time of 3 days. Earlier work suggests that 3 days is enough to dissipate the effect of initial conditions for simulations of the SoCAB [*Carreras-Sospedra et al*., 2006]. Boundary conditions for halocarbons were set constant along the perimeter of the modeling region at the background levels determined in Table 2.

[32] In the CMAQ model, halocarbon and CO emissions are assumed to be collocated, an important assumption in the tracer ratio method. This assumption is supported if modeled and measured concentration patterns are similar. The CMAQ model is not expected to reproduce the observed concentrations exactly because the CARB CO emission fields are not specific to the days during the CalNex study. In addition, field measurements are highly localized while the CMAQ model calculates concentrations averaged over 4 km $\times$ 4 km cells; point sources become diluted over large regions. However, the modeled and observed concentrations should be similar when examining regional averages if the collocation assumption and the meteorology are valid.

[33] A gauge of model performance is included in Figure 5, which shows correlation plots for the six HCFCs and HFCs examined in this study. For all species, we observe that the data points are distributed fairly evenly about the 1:1 line for most halocarbons. Only HCFC-141b has a group of data points that shows high observed concentrations with corresponding low modeled concentrations. This result could indicate the presence of an HCFC-141b plume that is not captured by the model due to the method for the spatial allocation of halocarbons. Considering observed concentrations are obtained at points in space and the model calculates concentration averages over 4 km $\times$ 4 km regions, some discrepancies between observed and modeled results are to be expected.

[34] Supplementary Figures 7 and 8 compare the modeled and observed halocarbon concentrations in the SoCAB on a per day and per hour basis, respectively. A more quantitative evaluation of model performance in the SoCAB is obtained by calculating the mean normalized bias (MNB) and mean normalized gross error (MNGE),

$$\mathrm{MNB} = \frac{1}{N}\sum_{i=1}^{N}\frac{C_M(x_i,t) - C_O(x_i,t)}{C_O(x_i,t)}, \tag{1}$$

$$\mathrm{MNGE} = \frac{1}{N}\sum_{i=1}^{N}\frac{|C_M(x_i,t) - C_O(x_i,t)|}{C_O(x_i,t)}, \tag{2}$$

where N is the number of observations in the region of interest during the campaign, $C_O(x_i,t)$ is the concentration of the ith observation, and $C_M(x_i,t)$ is the corresponding modeled concentration at the same position and time. These metrics are recommended by the USEPA for model

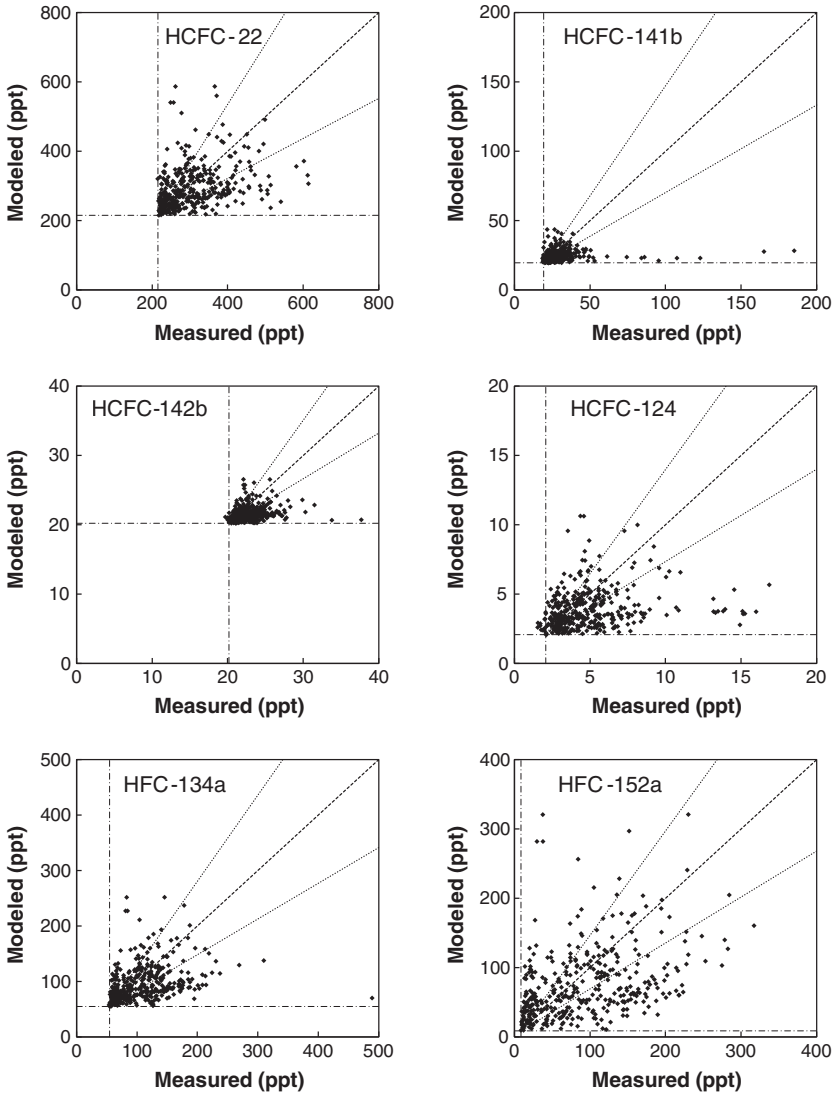

Figure 5. Comparison of modeled versus measured halocarbon mixing ratios in the South Coast Air Basin of California at altitudes less than 2000 m. The thick lines represent a modeled:measured ratio of 1:1 and modeled/measured ratios of 1:0.5 and 0.5:1. The two dashed lines illustrate the background levels.

evaluation [*USEPA*, 2007] and have been used extensively in the literature [*Russell and Dennis*, 2000; *Eder and Yu*, 2006; *Appel et al*., 2008; *Foley et al*., 2010]. It should be noted that the values of MNB and MNGE tend to be lower when background mixing ratios are high relative to emissions. For this reason, the MNB and MNGE are only calculated for HCFC-124, HFC-134a, and HFC-152a, which have an average mixing ratio in the SoCAB at least 2 times greater than background levels. We refrain from performing a quantitative assessment of the model performance for HCFC-141b, HCFC-142b, and HCFC-22 with the proposed metrics because of the high contribution of background levels on the observed mixing ratios. Supplementary Table 1 shows that the MNB and MNGE of HFC-124 and HFC-134a are within the acceptable performance criteria of less than $\pm$15% for MNB and less than 35% for MNGE [*Russell and Dennis*, 2000]. However, HFC-152a exceeds the performance criteria with an MNB of 33% and an MNGE of 66%. The high error of HFC-152a may result from the variability in measured concentrations as HFC-152a has the highest standard deviation and the greatest ratio of mean:background concentrations among the six halocarbons examined in this study (Table 2).

4. Summary and Conclusions

[35] Air samples were collected over California during the CalNex campaign in May and June 2010 and analyzed for a wide variety of volatile organic compounds including six CFC replacement compounds (HFC-134a, HFC-152a, HCFC-22, HCFC-124, HCFC-141b, HCFC-142b). Results show that tropospheric mixing ratios of HFC-134a, HFC-152a, HCFC-22, and HCFC-142b were enhanced over three major source regions—the South Coast Air Basin of California, San Joaquin Valley, and Sacramento Valley (Table 2)—compared to inflow levels. HCFC-141b was elevated only in the SoCAB, while high levels of HCFC-124 were observed in both the SoCAB and the SV.

[36] Halocarbon emission rates for the year 2010 were calculated for the SoCAB region based on field measurements and extrapolated to the state of California (Table 1) using population data. The present study improves the GHG emissions inventory for California, accomplishing one of the major goals of the CalNex campaign by providing a baseline emission rate that will help future studies determine if HCFC and HFC mitigation strategies are successful.

[37] Emissions calculated in this study are consistent with CARB's bottom-up estimates as well as previous studies examining HFC-134a and HFC-152a emissions from California in 2008 [*Barletta et al*., 2011]. The results also indicate HCFC-141b emissions possibly increased in California during 2005–2010 [*Gentner et al*., 2010] despite a ban on producing and importing this compound in 2003.

[38] For estimating emissions of HCFCs and HFCs using the tracer ratio method, halocarbon and CO sources were assumed to be collocated. The validity of this assumption is supported by the strong correlation between halocarbon and CO concentrations observed in field measurements, and it is consistent with the results from a state-of-the-science air quality model.

[39] The present study can be used as a baseline for HCFC-22, HCFC-124, and HCFC-142b emission rates as historical trends in the emission rates of these species are not available for California or its greatest source region, the SoCAB.

[40] **Acknowledgments.** The authors would like to thank the NOAA-WP3 flight and support crew for their efforts during the field deployment. We also thank Brent Love and Gloria Liu for technical support (University of California, Irvine) and Joseph Farran from the Office of Information Technology (University of California, Irvine) for his continuous support with computing resources. This work was funded (in part) by the National Science Foundation (NSF Grant CHE-0909227).

References

Appel, K. W., S. J. Roselle, R. C. Gilliam, and J. E. Pleim (2010), Sensitivity of the Community Multiscale Air Quality (CMAQ) model v4.7 results for the eastern United States to MM5 and WRF meteorological drivers, *GMD*, *3*(1), 169–188.

Appel, K. W., P. V. Bhave, A. B. Gilliland, G. Sarwar, and S. J. Roselle (2008), Evaluation of the community multiscale air quality (CMAQ) model version 4.5: Sensitivities impacting model performance: Part II. Particulate matter, *Atmos. Environ.*, *42*(24), 6057–6066.

Barletta, B., P. Nissenson, S. Meinardi, D. Dabdub, F. S. Rowland, R. A. VanCuren, J. Pederson, G. S. Diskin, and D. R. Blake (2011), HFC-152a and HFC-134a emission estimates and characterization of CFCs, CFC replacements, and other halogenated solvents measured during the 2008 ARCTAS campaign (CARB phase) over the South Coast Air Basin of California, *Atmos. Chem. Phys.*, *11*, 2655–2669, doi:10.5194/acp-11-2655-2011.

Barletta, B., et al. (2009), Characterization of volatile organic compounds (VOCs) in Asian and north American pollution plumes during INTEX-B: identification of specific Chinese air mass tracers, *Atmos. Chem. Phys.*, *9*, 5371–5388, doi:10.5194/acp-9-5371-2009.

Barnes, D. H., S. C. Wofsy, B. P. Fehlau, E. W. Gottlieb, J. W. Elkins, G. S. Dutton, and S. A. Montzka (2003), Urban/industrial pollution for the New York City–Washington, D. C., corridor, 1996–1998: 2. A study of the efficacy of the Montreal Protocol and other regulatory measures, *J. Geophys. Res.*, *108*, 4186, doi:10.1029/2001JD001116.

Boucouvala, D. and R. Bornstein (2003), Analysis of transport patterns during an SCOS97-NARSTO episode, *Atmos. Environ.*, *37*(supplement 2), S73–94. http://dx.doi.org/10.1016/S1352-2310(03)00383-2.

Byun, D.W., and J. K. S. Ching (1999), Science algorithms of the EPA Models-3 Community Multiscale Air Quality (CMAQ) Modeling System, *U.S. EPA/600/R-99/030*.

California Air Resources Board (2008), Climate Change Scoping Plan, A Framework for Change December 2008, Pursuant to AB 32 The California Global Warming Solutions Act of 2006.

Carreras-Sospedra, M., Rodriguez, M., Brouwer, J., and Dabdub D., (2006). Air quality modeling of the South Coast Air Basin of California: What do numbers really mean?, *J. Air Waste Manage. Assoc.*, *56*, 1184–1195.

Chang, J.S., R.A. Brost, I.S.A. Isaksen, S. Madronich, P. Middleton, W.R. Stockwell, and C.J. Walcek (1987), A three-dimensional Eulerian acid deposition model: Physical concepts and formulation, *J. Geophys. Res.*, *92*, 14,681–700, doi:10.1029/JD092iD12p14681.

Derwent, R.G., P.G. Simmonds, B.R. Greally, S. O'doherty, A. McCulloch, A. Manning, S. Reimann, D. Folini, and M. K. Vollmer (2007), The phase-in and phase-out of European emissions of HCFC-141b and HCFC-142b under the Montreal Protocol: evidence from observations at Mace Head, Ireland and Jungfraujoch, Switzerland from 1994 to 2004, *Atmos. Environ.*, *41*, 757–767, doi:10.1016/j.atmosenv.2006.09.009.

Eder, B., and Yu, S. (2006), A performance evaluation of the 2004 release of Models-3 CMAQ, *Atmos. Environ.*, *40*, 4811–4824, doi:10.1016/j.atmosenv.2005.08.045.

European Parliament (EP) (2006), Directive 2006/40/EC of the European Parliament and of the Council, relating to emissions from air-conditioning systems in motor vehicles and amending Council Directive, *70/156/EEC*, May 17, 2006.

Environmental Protection Agency (EPA) (2012), Inventory of U.S. greenhouse gas emissions and sinks: 1990–2009, Report EPA 430-R-12-001, U.S. UPA, Washington, DC, April 15, 2012.

Foley, K. M., et al. (2010), Incremental testing of the Community Multiscale Air Quality (CMAQ) modeling system version 4.7. *GMD*, *3* (1), 205–226.

Forster, P. M. de F., and M. J. Joshi (2005), The role of halocarbons in the climate change of the troposphere and stratosphere, *Clim. Change*, *71*, 1–2, 249–266, doi:10.1007/s10584-005-5955-7.

Forster, P., et al. (2007), Changes in Atmospheric Constituents and in Radiative Forcing, in *Climate Change 2007: The Physical Science Basis. Contribution of Working Group I to the Fourth Assessment Report of the Intergovernmental Panel on Climate Change*, edited by Solomon, S., Qin, D., Manning, M., Chen, Z., Marquis, M., Averyt, K. B., Tignor M., and Miller H. L., Cambridge University Press, Cambridge, United Kingdom and New York, NY, USA.

Gentner, D. R., A. M. Miller, and A. H. Goldstein (2010), Seasonal variability in anthropogenic halocarbon emissions, *Environ. Sci. Technol.*, *44*(14), 5377–5382, doi:10.1021/es1005362.

Greally, et al. (2007), Observations of 1,1-difluoroethane (HFC-152a) at AGAGE and SOGE monitoring stations in 1994–2004 and derived global and regional emission estimates, *J. Geophys. Res.*, *112*, D06308, doi:10.1029/2006JD007527.

Hass, H., H.J. Jacobs, M. Memmescheimer, A. Ebel, and J.S. Change (1991), Simulation of a wet deposition case in Europe using the European Acid Deposition Model (EURAD), *Nato-Chal M*, Vol. *VIII*, edited by van Dop H., and D.G. Steyn, Plenum Press, 205–213.

Henne, S., D. E. Shallcross, S. Reimann, P. Xiao, D. Brunner, S. O'Doherty, and B. Buchmann (2012), Future emissions and atmospheric fate of HFC-1234yf from mobile air conditioners in Europe, *Environ. Sci. Technol.*, *46* (3), 1650–1658, doi: 10.1021/es2034608.

Holloway, J. S., R. O. Jakoubek, D. D. Parrish, C. Gerbig, A. Volz-Thomas, S. Schmitgen, A. Fried, B. Wert, B. Henry, and J. R. Drummond (2000), Airborne intercomparison of vacuum ultraviolet fluorescence and tunable diode laser absorption measurements of tropospheric carbon monoxide, *J. Geophys. Res.*, *105*(D19), 24,251–24,261, doi:10.1029/2000JD900237.

Huang, M., et al. (2011), Multi-scale modeling study of the source contributions to near-surface ozone and sulfur oxides levels over California during the ARCTAS-CARB period, *Atmos. Chem. Phys.*, *11*, 3173–3194, doi:10.5194/acp-11-3173-2011.

Hurst, D. F., J. C. Lin, P. A. Romashkin, B. C. Daube, C. Gerbig, D. M. Matross, S. C. Wofsy, B. D. Hall, and J. W. Elkins (2006), Continuing global significance of emissions of Montreal Protocol-restricted halocarbons in the United States and Canada, *J. Geophys. Res.*, *111*, D15302, doi:10.1029/2005JD006785.

Hsu, Y.-K., T. VanCuren, S. Park, C. Jakober, J. Herner, M. FitzGibbon, D. R. Blake, and D. D. Parrish (2010), Methane emissions inventory verification in southern California, *Atmos. Environ.*, *44*(1), 1–7, 10.1016/j.atmosenv.2009.10.002.

Li, J., D. M. Cunnold, H.-J. Wang, R. F. Weiss, B. R. Miller, C. Harth, P. Salameh, and J. M. Harris (2005), Halocarbon emissions estimated from advanced global atmospheric gases experiment measured pollution events at Trinidad Head, California, *J. Geophys. Res.*, *110*, D14308, 10.1029/2004JD005739.

Liu, H., D. J. Jacob, I. Bey, R. M. Yantosca, B. N. Duncan, and G. W. Sachse (2003), Transport pathways for Asian pollution outflow over the Pacific: interannual and seasonal variations, *J. Geophys. Res.*, *108, D20*, 8786, doi:10.1029/2002JD003102.

Logan, J. A., M. J. Prather, S. C. Wofsy, and M. B. McElroy (1981), Tropospheric chemistry: a global perspective, *J. Geophys. Res.*, *86*, 7210–7254, doi:10.1029/JC086iC08p07210.

McCulloch, A., P. Ashford, and P. M. Midgley (2001), Historic emissions of fluorotrichloromethane (CFC-11) based on a market survey, *Atmos. Environ.*, *35*, 4387–4397, http://dx.doi.org/10.1016/S1352-2310(01)00249-7.

McCulloch, A., P. M. Midgley, and P Ashford (2003), Releases of refrigerant gases (CFC-12, HCFC-22 and HFC-134a) to the atmosphere, *Atmos. Environ.*, *37*, 889–902, http://dx.doi.org/10.1016/S1352-2310(02)00975-5.

Miller, B.R., J. Huang, R.F. Weiss, R.G. Prinn and P.J. Fraser (1998), Atmospheric trend and lifetime of chlorodifluoromethane (HCFC-22) and the global tropospheric OH concentrations, *J. Geophys. Res.*, *103*, 13,237–13,248, doi:10.1029/98JD00771.

Millet, D. B., and A. H. Goldstein (2004), Evidence of continuing methylchloroform emissions from the United States, *Geophys. Res. Lett.*, *31*, L17101, doi:10.1029/2004GL020166.

Millet, D. B., E. L. Atlas, D. R. Blake, N. J. Blake, G. S. Diskin, J. S. Holloway, R. C. Hudman, S. Meinardi, T. B. Ryerson, and G. W. Sachse (2009), Halocarbon emissions from the United States and Mexico and their global warming potential, *Environ. Sci. Tech.*, *43*, 1055–1060, doi:10.1021/es802146j.

O'Doherty, S., et al. (2004), Rapid growth of hydrofluorocarbon 134a and hydrochloro-fluorocarbons 141b, 142b, and 22 from Advanced Global Atmospheric Gases Experiment (AGAGE) observations at Cape Grim, Tasmania, and Mace Head, Ireland, *J. Geophys. Res.*, *109* (D6), D06310, 10.1029/2003JD004277.

Papasavva, S., D. J. Luecken, R. L. Waterland, K. N. Taddonio, and S. O. Andersen (2009), Estimated 2017 refrigerant emissions of 2,3,3,3-tetrafluoropropene (HFC-1234yf) in the United States resulting from automobile air conditioning, *Environ. Sci. Technol.*, *43*, 9252–9259, doi:10.1021/es902124u.

Prinn, R.G., et al. (2000), A history of chemically and radiatively important gases in air deduced from ALE/GAGE/AGAGE, *J. Geophys. Res.*, *105*, 17751–17792, doi:10.1029/2000JD900141.

Reimann, S., et al. (2005), Low European methyl chloroform emissions inferred from long-term atmospheric measurements, *Nature*, *433*, 506–508, doi:10.1038/nature03220.

Russell A., and Dennis R. (2000), NARSTO critical review of photochemical models and modeling. *Atmos. Environ.*, *34*, 2283–2324, http://dx.doi.org/10.1016/S1352-2310(99)00468-9.

Sihra, K., M. D. Hurley, K. P. Shine, and T. J. Wallington (2001), Updated radiative forcing estimates of 65 halocarbons and nonmethane hydrocarbons, *J. Geophys. Res.*, *106*(D17), 20,493–20,505, doi:10.1029/2000JD900716.

Skamarock, W. C., N. J. Klemp, J. Dudhia, D. O. Gill, D. M. Barker, W. Wang, and J. G. Powers (2005), A Description of the Advanced Research WRF Version 2. NCAR technical note NCAR/TN-468 + STR.

Stohl, A., et al. (2009), An analytical inversion method for determining regional and global emissions of greenhouse gases: Sensitivity studies and application to halocarbons, *Atmos. Chem. Phys.*, *9*, 1597–1620, doi:10.5194/acp-9-1597-2009.

Sturrock, G. A., D. M. Etheridge, C. M. Trudinger, P. J. Fraser, and A. M. Smith (2002), Atmospheric histories of halocarbons from analysis of Antarctic firn air: Major Montreal Protocol species, *J. Geophys. Res.*, *107*, 4765–4778, doi:10.1029/2002JD002548.

United Nations Environment Programme (UNEP) (2003), *Handbook for the International treaties for the protection of the ozone layer*, 6th edition, Nairobi, Kenya.

United States Environmental Protection Agency (USEPA) (2007), Guidance on the Use of Models and Other Analyses for Demonstrating Attainment of Air Quality Goals for Ozone, PM2.5, and Regional HazeOffice of Air Quality Planning and Standards, Air Quality Analysis Division, Air Quality Modeling Group, EPA-454/B-07-002, April 2007. Research Triangle Park, North Carolina, USA.

WMO (World Meteorological Organization) (2011), Scientific assessment of ozone depletion: 2010, Global Ozone Research and Monitoring Project Report No. 52, Geneva, Switzerland.

Yamartino, R. J. (1993), Nonnegative, conserved scalar transport using grid-cell-centered, spectrally constrained Blackman cubics for applications on a variable-thickness mesh. *Mon. Wea. Rev.*, *121*, 753–763.

Yokouchi, Y., S. Taguchi, T. Saito, Y. Tohjima, H. Tanimoto, and H. Mukai (2006), High frequency measurements of HFCs at a remote site in east Asia and their implications for Chinese emissions, *Geophys. Res. Lett.*, *33*, L21814, doi:10.1029/2006GL026403.

Zaremba, L. L., and J. J. Carroll (1999), Summer Wind Flow Regimes over the Sacramento Valley. *J. Appl. Meteorol.*, *38*, 1463–1473.

Zhong, S., C. D. Whiteman, and X. Bian (2004), Diurnal Evolution of Three-Dimensional Wind and Temperature Structure in California's Central Valley. *J. Appl. Meteorol.*, *43*, 1679–1699.